

C. Cornaro¹

Department of Enterprise Engineering,
University of Rome "Tor Vergata",
Via del Politecnico 1, Rome 00133, Italy;
CHOSE,
University of Rome "Tor Vergata",
Via del Politecnico 1, Rome 00133, Italy
e-mail: cornaro@uniroma2.it

F. Bucci

Department of Enterprise Engineering,
University of Rome "Tor Vergata",
Via del Politecnico 1, Rome 00133, Italy
e-mail: frabucci@gmail.com

M. Pierro

Department of Enterprise Engineering,
University of Rome "Tor Vergata",
Via del Politecnico 1, Rome 00133, Italy
e-mail: marco.pierro@gmail.com

F. Del Frate

Department of Civil Engineering and
Computer Science Engineering,
University of Rome "Tor Vergata",
Via del Politecnico 1, Rome 00133, Italy
e-mail: fabio.delfrate@disp.uniroma2.it

S. Peronaci

Department of Civil Engineering and
Computer Science Engineering,
University of Rome "Tor Vergata",
Via del Politecnico 1, Rome 00133, Italy
e-mail: simone.peronaci@hotmail.it

A. Taravat

Department of Civil Engineering and
Computer Science Engineering,
University of Rome "Tor Vergata",
Via del Politecnico 1, Rome 00133, Italy
e-mail: art23130@gmail.com

Twenty-Four Hour Solar Irradiance Forecast Based on Neural Networks and Numerical Weather Prediction

In this paper, several models to forecast the hourly solar irradiance with a day in advance using artificial neural network techniques have been developed and analyzed. The forecast irradiance is the one incident on the plane of the modules array of a photovoltaic plant. Pure statistical (ST) models that use only local measured data and model output statistics (MOS) approaches to refine numerical weather prediction data are tested for the University of Rome "Tor Vergata" site. The performance of ST and MOS, together with the persistence model (PM), is compared. The ST models improve the performance of the PM of around 20%. The combination of ST and NWP in the MOS approach gives the best performance, improving the forecast of approximately 39% with respect to the PM. [DOI: 10.1115/1.4029452]

Keywords: solar radiation, grid stability, photovoltaic, forecast, neural networks

1 Introduction

The forecast of the solar energy production is becoming a key issue for many countries that have to deal with a consistent amount of electricity produced by renewable sources. In particular, the 24/72 hr horizon forecast is essential for transmission scheduling and day ahead energy market. Also Italy, with its 16.7 GWh of photovoltaic (PV) energy production in 2012, is starting to deal with some criticisms of the integration of the PV plants into the national grid. In particular, the Italian regulatory system, in 2012, proposed a norm that provides a penalty if the PV production forecast is 15% higher than the real production in terms of normalized mean absolute error (MAE) between forecast and real data.

For these reasons, papers dealing with the forecast of solar energy for this specific application are growing fast in the literature.

In general, the techniques to forecast the solar radiation or PV production on the 24/72 hr horizon can be divided in three main groups [1,2]:

- (1) NWP models
- (2) ST models
- (3) MOS

The NWP models [3] are essentially based on the numerical integration of coupled differential equations that describe the dynamic of the atmosphere and radiations transport mechanisms.

This technique is based on deterministic physical models. Although they are very reliable models, however, they show two main problems: the nonlinearity of the used equations and the spatial resolution of the integration grid (from 100 km² to few km²) that is too wide with respect to the PV plants size. Inside the grid cell, the cloud cover and aerosols are considered as average values thus great errors could be induced both in the amount and in the time of the forecast irradiance at the PV site. Besides, many NWP models have a temporal output interval greater than 1 hr while, as in this case, the hourly irradiance forecast is required. Just to cite an example, Perez et al. [4] presented an extensive validation of short and medium term solar radiation forecast for various sites in the U.S.

The ST models are based on methods to reconstruct the relations between the hourly irradiance and past meteorological parameters (cloud ratio (CR), air temperature, relative humidity, pressure, etc.) or past irradiance observations. The most used models for the 1 day horizon irradiance forecast are based on

¹Corresponding author.

Contributed by the Solar Energy Division of ASME for publication in the JOURNAL OF SOLAR ENERGY ENGINEERING: INCLUDING WIND ENERGY AND BUILDING ENERGY CONSERVATION. Manuscript received March 28, 2014; final manuscript received December 18, 2014; published online January 8, 2015. Assoc. Editor: Philippe Blanc.

artificial neural networks (ANN). With this method, the forecast could be achieved by fast simple algorithms that use only local meteorological measurements [5–7] and ST feature parameters [8]. Thus, on one hand, ST models do not suffer from spatial and temporal resolution problems. On the other hand, they are not able to provide a good forecast in unstable weather conditions, since in these cases the correlation between the irradiance and the input variables rapidly falls down and consequently the models are not able to adequately learn in the training phase.

The MOS approach combines both NWP and ST models [9,10]. The first one is used for the forecast, while the second allows to correct the site effects through local measurements. A variety of MOS techniques, which use ST postprocessing of the NWP output and stochastic learning techniques, have been developed by various authors. An ST postprocessing correction of the bias errors of the European Centre for Medium-Range Weather Forecast (ECMWF)-NWP data was proposed in Ref. [11]. This seems to be the most performing MOS for global irradiance forecast as evidenced in Ref. [12].

Most of the papers in the literature that explore the use of ANN with MOS techniques are focused on the solar irradiance forecast, however, some authors use ANN with MOS also to directly forecast the PV plant production as it can be found in Refs. [10], [13], and [14]. Most of the examined literature that uses ANN and/or MOS techniques with ANN is referred to analysis and forecast over few days data samples and not on a year (that is usually the used benchmark period), so it is not easy to make a direct comparison of the results obtained by other authors. The intent of this work is to evaluate the forecast potentiality of ST and MOS based on ANN and NWP with a horizon of 24 hr for the site of Rome using almost 2 yr of data available at the ESTER lab of the University of Rome “Tor Vergata.” The NWP data used in the MOS come from the ECMWF [15]. The results, obtained by four ST models based on different kinds of neural networks algorithms that use only in situ measurements, are reported. The forecasts obtained by four different MOS, which use NWP data and local measurements as input of ANN, are also analyzed. It appears that the deterministic and statistic approaches have different sources of errors in their forecasting outputs and the combination of the two can sensibly improve the forecast performance. Thus, all the MOS techniques provide similar and better results.

It should be remarked that the majority of the works in the forecasting literature provide the prediction of the global horizontal irradiance (GHI) while to forecast the PV energy production the irradiance on the POAs is required. Thus, the transposition factor from the horizontal plane to POA introduces an additional error in the forecast. For this reason, all the presented models directly provide the forecast of the POA irradiance.

2 Data Description

2.1 Local Experimental Data and Preprocessing. The local experimental data used as input and to train and test the models come from the ESTER outdoor Laboratory—University of Rome “Tor Vergata” (41.18556 deg latitude north, 12.6233 deg longitude east, and altitude 100 m) [16]. The global irradiance used for the forecast is the one measured on the plane of PV modules (POA) exposed at ESTER lab from January 2009 to the end of October 2010. The tilt angle was changed every month to optimize the normal incidence at noon and the overall energy collection of the module during the month. In particular, the global and diffuse horizontal irradiance, the global POA irradiance, air temperature and the energy produced by a c-Si module (Kyocera KC 125) were measured each minute during the considered period. Irradiance was measured by three Kipp&Zonen CM21 pyranometers, while air temperature by a Rotronic thermohygrometer with 1-min time rate.

The data were filtered removing the not physically consistent measurements due to monitoring problems or instrument malfunctions.

According to Ref. [17], a quality control procedure was applied based on a plausible value check and a time consistency check. The aim of the first check was to verify if the values of instantaneous data were within acceptable range limits:

- GHI: 0 W/m² to 1600 W/m²
- Diffuse horizontal irradiance (DHI): 0 W/m² to 1600 W/m²
- Global POA irradiance (GPOA): 0 W/m² to 1600 W/m²
- Air temperature (Ta): –20 °C to 80 °C.

The first quality check removed 4688 records over 905,425 data (including night values).

The aim of the second check was to verify the rate of change of instantaneous data (detection of unrealistic jumps in values or “dead band” caused by blocked sensors). The persistence test and the step test were applied. In the persistence test, if the 1-min values did not vary over the past 60 min by more than the specified limit (a threshold value) then the current 1-min value failed the check. The threshold values were:

- Ta: 0.01 °C
- DHI: 0.01 W/m²
- GPOA and GHI: 0.02 W/m².

In the step test, if the current instantaneous value differed from the prior one by more than a specific limit (step), then the current instantaneous value failed the check. The limits were:

- Ta: 3 °C
- GPOA, GHI, DHI: 1000 W/m².

The second quality check removed 4381 records over 905,425 data (including night values).

For each day, data reconstruction by linear interpolation was applied if no more than 60 consecutive missing samples were encountered; otherwise, the whole day was removed from the data set. After this operation, the hourly and monthly data were calculated.

The data reconstruction was introduced to overcome the data monitoring system faults that bring to underestimation of the produced energy.

At the end of the preprocessing, a total of 124 days over 2 yr (2009 and 2010) were missing or discarded.

2.2 NWP Data. The NWP data are the output of the ERA-INTERIM model that is the latest global atmospheric reanalysis software produced by the ECMWF [15]. In particular, they consist of a 24 hr horizon forecast of the horizontal global solar radiation. The spatial resolution of these data correspond to a cell of 13.5 km × 13.5 km side (0.125 deg × 0.125 deg), the maximum available resolution. The temporal output interval is 3 hr; thus, for each day, the data contain eight forecasts of the cumulative integral of horizontal global irradiance starting from midnight UTC. According to the local measurements, the considered period is between the January 1, 2009 and October 31, 2010.

Almost all the developed ANN models used the daily irradiation as input, thus the NWP time resolution was not a concern. As it will be described later in the paper, only one model used the hourly forecast irradiance thus to obtain these values a linear interpolation over the average 3 hr irradiance was performed. This simple procedure is less accurate than the interpolation of the clear sky index as pointed out by Ref. [11], nevertheless, the ANN model was able to correct this further systematic error.

3 Models Input Parameters

Since the final objective of the work is to forecast the PV energy production, all the inputs of the reported forecasting models should be variables that are commonly measured by the medium–large size PV plant monitoring systems. Besides, these parameters need to be strongly correlated to the irradiance of the day ahead; as proven by other authors that made sensitivity analysis [7] or used dedicated algorithms for input selection [18].

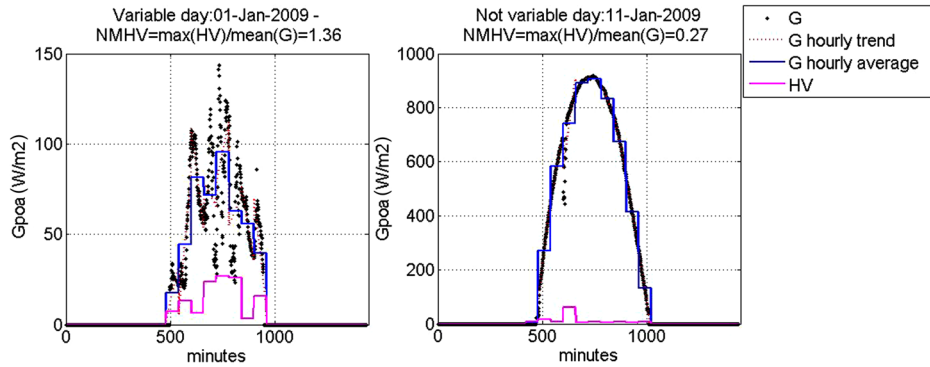


Fig. 1 HV of irradiance for two different days. Variable day: January 1, 2009 and not variable day: January 11, 2009.

Moreover, also two ST parameters similar to the one used by Ref. [8] were considered in this study to verify the possibility of forecast improvement.

For each day, the hourly solar irradiance features (G_{poa_1} – $G_{poa_{24}}$), to be forecasted, have been characterized by the following five parameters:

- OD = ordinal day
- H_h and H_{poa} = daily global irradiation on horizontal and POA (kWh/m^2)
- CR = cloud ratio
- NMHV = normalized maximum hourly variation of the solar irradiance
- NADV = normalized absolute daily variation of the solar radiation between the day (t) and the day ($t - 1$).

The OD takes into account for the yearly variations of sunrise and sunset hours.

The H_h and H_{poa} are the integral of hourly solar irradiance and depict both the yearly solar energy variation and meteorological features of the day. Besides, the H_{poa} takes into account orientation and tilt of the PV plane.

The CR is defined as the ratio between the horizontal diffuse (H_{sh}) and global (H_h) daily irradiation

$$CR = \frac{H_{sh}}{H_h} \quad (1)$$

This parameter is strictly related to the stochastic meteorological conditions. For $CR < 0.4$, the day could be considered clear while $CR > 0.4$ indicates overcast days. It requires specific measurements of the diffuse irradiance that are not always available at the PV plant, but for practical applications it could be replaced by the clearness index K_t , defined as the ratio between the global irradiance on the horizontal plane at the ground and the extra atmospheric irradiance evaluated on the horizontal plane. Also the clear sky index (K_{cs}) in which the extra atmospheric irradiance is substituted by the clear sky model can be a good indicator of the weather conditions.

The NMHV of the solar irradiance is a new index defined by the authors and is written as

$$NMHV = \frac{\max_h \left\{ \sqrt{\frac{\sum_{\min=1}^{60} (G_h^{\min} - \text{fit}(G_h^{\min}))^2}{60}} \right\}}{\langle G_h^{\min} \rangle_{\text{day}}} \quad (2)$$

where G_h^{\min} = irradiance at minute \min of the hour h (W/m^2), $\text{fit}(G_h^{\min})$ = linear fit of G_h^{\min} (W/m^2), and $\langle G_h^{\min} \rangle_{\text{day}}$ = daily average irradiance (W/m^2)

The NMHV is calculated fitting the data inside each hour with a linear trend ($\text{fit}(G_h^{\min})$) and then evaluating the root mean square

(RMS) between the fit results and the real data (G_h^{\min}). NMHV is the maximum value of hourly RMS calculated in the day, normalized by the average daily irradiance ($\langle G_h^{\min} \rangle_{\text{day}}$). This ST parameter represents the maximum fluctuation of the measured irradiance around the hourly linear trend with respect to the daily average irradiance and it is used to describe the daily variability of the irradiance. In clear sky days, it could be near to zero while in high variable days it could reach the value of 2 (fluctuations are two times the mean daily irradiance). Variable days have $NMHV > 0.4$. Figure 1 shows the HV daily behavior for a variable and a not variable day.

The NADV of the solar irradiation is also a new index defined by the authors and is written as

$$NADV = |NDV| = \left| \frac{(H(t) - H(t - 1))}{(H(t) + H(t - 1))/2} \right| \quad (3)$$

where

$$H(t) \text{ and } H(t - 1) = \text{irradiations at days: } t \text{ and } t - 1$$

It is used as an indicator of the weather persistence of 1 day with respect to the other. $NADV < 0.4$ has been considered as indicator of stable weather conditions with respect to the past day. To characterize the day by day variability of the site, a 5 yr dataset (2008–2012) coming from the weather and solar station of ESTER facility was considered. Figure 2 shows the probability density function (PDF) of NDV of the horizontal irradiation, measured at the ESTER location during the considered years. It can be observed that small variations of weather conditions between two consecutive days (low NADV) are much more probable than fast weather changing (high NADV). In general, the mean value and

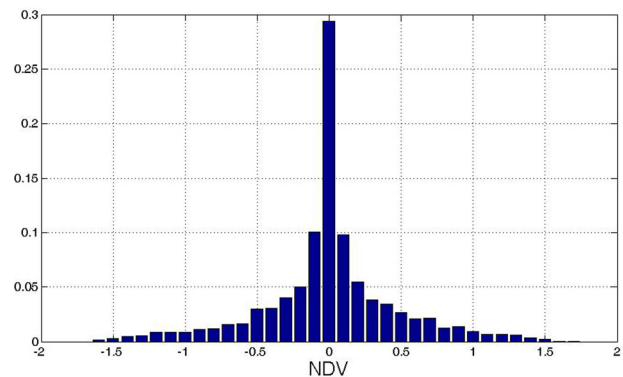


Fig. 2 PDF of normalized daily variation

Table 1 Pearson correlations of the input variables at lag0 and Hpoa at lag1 in the year 2009

	Hpoa (lag0)	Ta (lag0)	CR (lag0)	NMHV (lag0)	NADV (lag0)
Hpoa(lag1)	49%	51%	40%	19%	30%

the variance of PDF changes from year to year and from site to site but the shape of the PDF remains the same. Thus the weather tends to be persistent.

Also for this reason, to evaluate a forecast model performance, the persistence model (PM) is commonly used. Moreover, fast weather perturbations (high NADV) could be forecast only using NWP models since the correlations between the input parameters at lag0 (day t) and the forecast irradiance at lag1 (day $t + 1$) are very low. Nevertheless, the ST models could show good performance for the majority of the days that have relatively persistent conditions (low NADV).

In order to strengthen the input variables choice, the correlation between them at the same day (lag0) and the daily irradiation on the plane of array (Hpoa) of the day ahead (lag1) was evaluated. The Pearson correlation coefficients for the five variables are listed in Table 1. High correlation coefficients can be observed for all the variables proving that they all contribute as significant inputs of the ST models. However, the two ST parameters show lower correlation coefficients than the other physical variable indicating a minor contribution to the solar irradiance forecast. Another meteorological parameter that is usually measured by all the PV plant monitoring systems is the ambient temperature (Ta). Since it is strongly correlated to the daily irradiation (see Table 1), it was used as input variable.

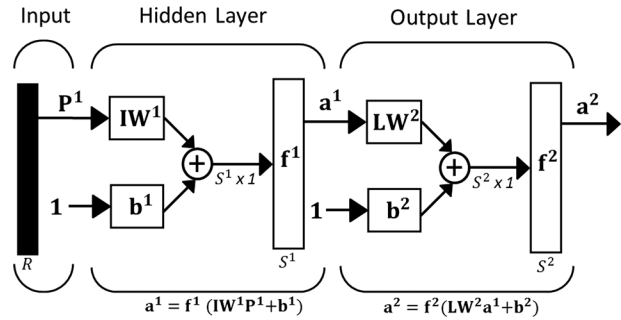


Fig. 3 Sketch of the MLPNN architecture. P^1 : input vector with R rows. For i -layer, IW^i : input weights, LW^i : layer weights, b^i : bias vector, S^i : number of neurons, a^i : output vector, and f^i : transfer function.

4 Forecast Models Description

In this section, the general features of all the used forecast models are discussed. In Table 2, all the technical specifications of each model and technique are reported.

4.1 PM. Since the weather tends to be persistent, it is possible to define a trivial model [19]

$$[Gpoa_1(t + 1), \dots, Gpoa_{24}(t + 1)] = [Gpoa_1(t), \dots, Gpoa_{24}(t)] \quad (4)$$

Table 2 Technical specifications of the models

Type	Name	Description
Persistence	PM	$[Gpoa_1(t + 1) \dots Gpoa_{24}(t + 1)] = [Gpoa_1(t) \dots Gpoa_{24}(t)]$
ST models with feed forward multi layer perceptron	1MLP	$[Gpoa_1(t + 1) \dots Gpoa_{24}(t + 1)] = f1(OD(t), Hpoa(t), Ta(t), CR(t))$ JAVANNIS: $R = 6, S^1 = 30, f^1 = \text{tansigmoid}, S^2 = 24, f^2 = \text{purelinear}, \text{BBP}$
	2MLP	$[Gpoa_1(t + 1) \dots Gpoa_{24}(t + 1)] = f2(OD(t), Hpoa(t), Ta(t), CR(t), NMHV(t), NADV(t))$ JAVANNIS: $R = 6, S^1 = 30, f^1 = \text{tansigmoid}, S^2 = 24, f^2 = \text{purelinear}, \text{BBP}$
	3MLP	Four seasonal NN in parallel: $[Gpoa_1(t + 1) \dots Gpoa_{24}(t + 1)] = f3(OD(t), Hpoa(t), Ta(t), CR(t), NMHV(t), NADV(t))$ JAVANNIS: $R = 6, S^1 = 30, f^1 = \text{tansigmoid}, S^2 = 24, f^2 = \text{purelinear}, \text{LMA}$
	4MLP2Net: MLP4.1	Two NN in series: $[Hpoa(t + 1)] = f4.1(OD(t - 1), Hpoa(t - 1), Ta(t - 1), CR(t - 1), OD(t), Hpoa(t), Ta(t), CR(t))$ MATLAB: $R = 8, S^1 = 10, f^1 = \text{tansigmoid}, S^2 = 1, f^2 = \text{purelinear}, \text{LMA}$
MOS technique with NWP and multi layer perceptron feed forward	MLP4.2	$[Gpoa_1(t + 1) \dots Gpoa_{24}(t + 1)] = f4.2(OD(t + 1), Hpoa(t + 1), Ta(t), CR(t), NHV(t), NDV(t))$ MATLAB: $R = 6, S^1 = 10, f^1 = \text{tansigmoid}, S^2 = 1, f^2 = \text{purelinear}, \text{LMA}$
	5NWPMLP	$[Gpoa_1(t + 1) \dots Gpoa_{24}(t + 1)] = f8(OD(t), Hpoa(t), Ta(t), CR(t), OD(t + 1), Hh_nwp(t + 1))$ MATLAB: $R = 6, S^1 = 10, f^1 = \text{tansigmoid}, S^2 = 15, f^2 = \text{purelinear}, \text{LMA}$
	6NWPMLP	$[Gpoa_1(t + 1) \dots Gpoa_{24}(t + 1)] = f9(OD(t + 1), [Gh_nwp_1(t + 1) \dots Gh_nwp_{24}(t + 1)])$ MATLAB: $R = 25, S^1 = 20, f^1 = \text{tansigmoid}, S^2 = 15, f^2 = \text{purelinear}, \text{LMA}$
	7NWPMLP	$[Gpoa_1(t + 1) \dots Gpoa_{24}(t + 1)] = f10(OD(t), Hpoa(t), Ta(t), CR(t), OD(t + 1), [Gh_nwp_1(t + 1) \dots Gh_nwp_{24}(t + 1)])$ MATLAB: $R = 25, S^1 = 20, f^1 = \text{tansigmoid}, S^2 = 15, f^2 = \text{purelinear}, \text{LMA}$
	8NWPMLP2Net: NWPMLP8.1	Two NN in series: $[Hpoa(t + 1)] = f41(OD(t - 1), Hpoa(t - 1), Ta(t - 1), CR(t - 1), OD(t), Hpoa(t), Ta(t), CR(t), OD(t + 1), Hh_nwp(t + 1))$ MATLAB: $R = 10, S^1 = 10, f^1 = \text{tansigmoid}, S^2 = 1, f^2 = \text{purelinear}, \text{LMA}$
	MLP4.2	$[Gpoa_1(t + 1) \dots Gpoa_{24}(t + 1)] = f42(OD(t + 1), Hpoa(t + 1))$ MATLAB: $R = 6, S^1 = 10, f^1 = \text{tansigmoid}, S^2 = 1, f^2 = \text{purelinear}, \text{LMA}$

Notes: LMA = Levenberg–Marquardt algorithm; BBP = batch back propagation; OD = ordinal date (ISO 8601); H = daily irradiance (kWh/m^2 day); CR = cloud ratio; Ta = mean daily temperature; NMHV = normalized maximum hour variation; and NADV = normalized absolute day variation.

A forecasting model should have better performance than the PM. Moreover, the performance improvement of a model with respect to the PM is a parameter almost yearly and site independent.

4.2 ANN Models. To develop the ST models and MOS technique, the ANN multilayer perceptron neural network (MLPNN) algorithm was used.

The MLPNN architecture, reported in Fig. 3, uses meteorological parameters to forecast the 1 day ahead hourly irradiance

$$[G_{\text{poa}_1}(t+1), \dots, G_{\text{poa}_{24}}(t+1)] = f(\text{meteorological parameters}) \quad (5)$$

The inputs meteorological parameters could come only from past local measurements (in the case of ST models) or also from NWP forecasting data (in the case of MOS).

In this work, the performance of eight different MLPNN used to develop ST and MOS, are reported. These ANN were developed with two softwares: MATLAB and JAVA NNS to verify the reliability of the models. Similar performance was found and the results of most performing models were reported.

To define the best numbers of neurons and optimize the network, the following procedure was used:

- 284 days selected from the November 1, 2009 to October 31, 2010 with the condition that three consecutive days data exist were used for training and validation. The 80% of these data

were randomly sorted for training the MLP and the 20% for validation.

- To select the best number of neurons of the hidden layer (best S^1) for each dimension $S^1 = [1,5,10,15,20,25,30]$, the NN was trained almost 20 times. Then the architecture that exhibits the minimum mean square error (MSE) on the validation set was chosen.
- To optimize the model (best IW¹ and LW), the selected NN architecture was trained almost 50 times, then, the MLP that presented the minimum MSE on the validation set was selected.
- To test the best model, the data of 270 days selected from the January 1, 2009 to December 31, 2009 were used with the condition that three consecutive days data should exist.

For the NN developed with MATLAB tool, the training algorithm is the Levenberg–Marquardt (LMA) [20], while for the one developed with JAVA NNS the training algorithm is the batch back propagation (BBP). For each training operations, the convergence process was stopped when the MSE on the validation set reached its minimum.

5 Results and Discussion

5.1 ST Performance Indicators. The main ST performance indicators used in the analysis are listed in Table 3. The Kolmogorov–Smirnov index (KS) is the maximum difference

Table 3 Main performance parameters used in the analysis

Name	Acronym and formulae
KS index	$KS = \sup_G CDF^m(G) - CDF^f(G) $
Pearson correlation coefficient	$CORR = \left(\frac{\sum_{i=1}^n (G_i^m - \bar{G}^m)(G_i^f - \bar{G}^f)}{\sqrt{\sum_{i=1}^n (G_i^m - \bar{G}^m)^2 \sum_{j=1}^n (G_j^f - \bar{G}^f)^2}} \right)$
RMSE	$RMSE = \sqrt{\frac{\sum_{i=1}^n (G_i^m - G_i^f)^2}{n}} \text{ (W/m}^2\text{)}$
MAE	$MAE = \left(\frac{\sum_{i=1}^n G_i^m - G_i^f }{n} \right) \text{ (W/m}^2\text{)}$
MBE	$MBE = \left(\frac{\sum_{i=1}^n G_i^m - G_i^f }{n} \right) \text{ (W/m}^2\text{)}$
Daily CAE	$CAE = \sum_{i=1}^{24} G_i^m - G_i^f \text{ (kWh/m}^2\text{day)}$
Improvement or skill score	$I_{RMSE} = 100 \left(\frac{RMSE(PM) - RMSE(model)}{RMSE(PM)} \right) \text{ (\%)}$
NMAE difference	$D_{NMAE} = NMAE(PM) - NMAE(model) \text{ (\%)}$

Note: G_i^m = measured hourly irradiance (kW/m²); G_i^f = forecast hourly irradiance (kW/m²).

Table 4 Models performance main results, Gpoa is the global irradiance on the plane of the module. Boldface values are referred to the best models results in terms of performance and reliability.

Forecast variable	Name	Test days	KS	CORR	RMSE (W/m ²)	NRMSE (%)	I_{RMSE} (%)	NMAE (%)	D_{NMAE} (%)	
Gpoa	PM	270	0	0.72	236	50.6	1	29.6	1	
	ST models with local data									
	1MLP	270	0.13	0.81	188	40.2	20.6	29.1	0.5	
	2MLP	270	0.09	0.79	197	42.3	17.1	28.4	1.2	
	3MLP	270	0.05	0.72	231	49.6	2.4	32.9	-3.3	
	4MLP2Net	270	0.09	0.81	187	40.1	21.3	27.4	2.2	
	MOS models with local and NWP data									
	5NWPMLP	270	0.06	0.89	145	31	38.7	20.2	9.4	
	6NWPMLP	270	0.06	0.89	145	31.2	38.4	20.9	8.7	
	7NWPMLP	270	0.05	0.89	147	31.5	37.9	20.7	8.9	
	8NWPMLP2Net	270	0.07	0.884	149	31.9	37.2	20.8	8.8	

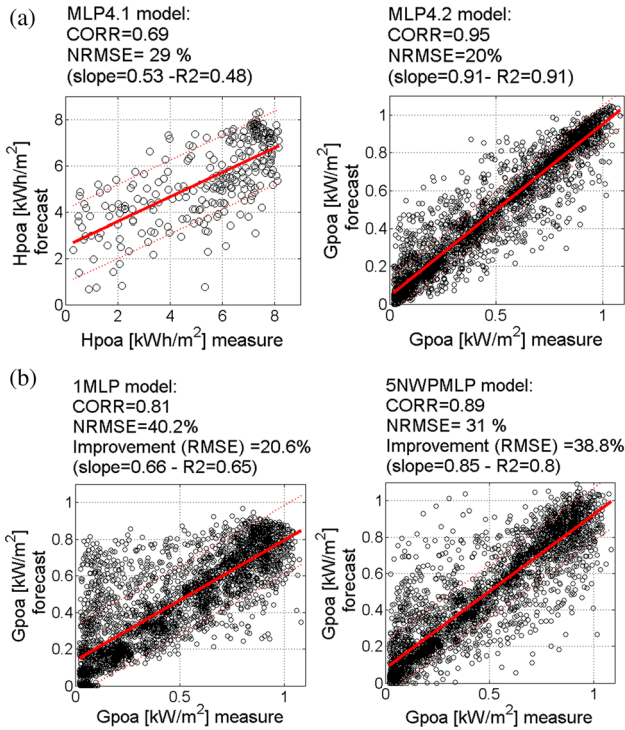


Fig. 4 (a) correlations between measured data and MPL4.1 and MPL4.2 model forecast data (hourly shape forecasting), (b) correlations between measured data and 1MLP and 5NWPMLP

between the cumulative density function (CDF) of the measured and forecast irradiance. It evaluates the similarity between the two irradiance distribution functions (measured and forecast). The normalized values of RMSE and MAE are evaluated dividing the parameters by the yearly average irradiance.

All the ST indexes are calculated considering only the day time hourly irradiance ($G > 20 \text{ W/m}^2$), indeed including the nighttime values all the average calculations would be underestimated.

It should also be pointed out that the NMAE is exactly the measure of the unbalanced energy with respect to the total PV electricity delivered to the grid. Even if, in the literature, the most used indicator is the RMSE, also the NMAE evaluation is very important.

5.2 Models Performance Analysis. The main results of all the forecast models are summarized in Table 4.

The performance of four ST models developed with MLPNN architecture was analyzed. The model 2MLP uses as input, all the daily variables described in Sec. 3, while the model 1MLP uses only the parameters OD, H_h , CR, and Ta that have the maximum correlation with daily irradiance at day $t + 1$ (lag1) (Table 1). The model 1MLP shows the best performance proving the right minimum choice of the input variables and confirming the result obtained in Ref. [5]. Figure 4 shows the scatter plot of this model. The model 3MLP explores a seasonal approach, thus for each season an MLPNN was developed and used in parallel. Even if this approach could potentially bring to good results, one season is insufficient to train and validate each ANN. Thus, in this case, the 3MLP model shows worst performance with respect to the others.

Noting that the correlation between the measured daily irradiation (H_{poa}) at lag0 and lag1 is greater than the one between hourly irradiance (G_{poa}) at lag0 and lag1, the forecast problem was split in two steps, using two NN in series: one (MLP4.1) to forecast the $H_{poa}(t + 1)$ and other (MLP4.2) to reconstruct the G_{poa} from the forecast daily irradiation ($H_{poa}(t + 1)$). The model 4MLP2Net summarizes the results of this two steps approach.

The MLP4.2 that predicts the hourly irradiance from the same day irradiance (shape irradiance forecast model) shows very good performance (Corr = 0.95, NRMSE = 20%, and NMAE = 13%, see Fig. 4).

Nevertheless, the first step MLP4.1 is not a well enough performing model (Corr = 0.69, NRMSE = 29%, and NMAE = 23%, see Fig. 4). Besides, for the MLP4.1 model, an over fitting trend in the training phase was observed, thus even if the 4MLP model shows the best performance, this model was considered less reliable than the others. Probably, this ANN model could be improved using more than 1 yr data for training and validation.

Almost all ST models realize an improvement of around 20% in terms of RMSE but they do not achieve any gain in terms of MAE (imbalanced energy measure).

Finally, it should be remarked that there is not a general standard for ST NN model performance evaluation in the literature: different ST indicators and test time intervals are used or different variables are forecast (horizontal, POA irradiance, and PV power). Thus, as already pointed out, the 1 yr results (270 days spread over 1 yr) presented in this article are not easily comparable with the ones reported in the literature [6–8, 10, 13]. Moreover, a systematic study on the performance improvement dependence on

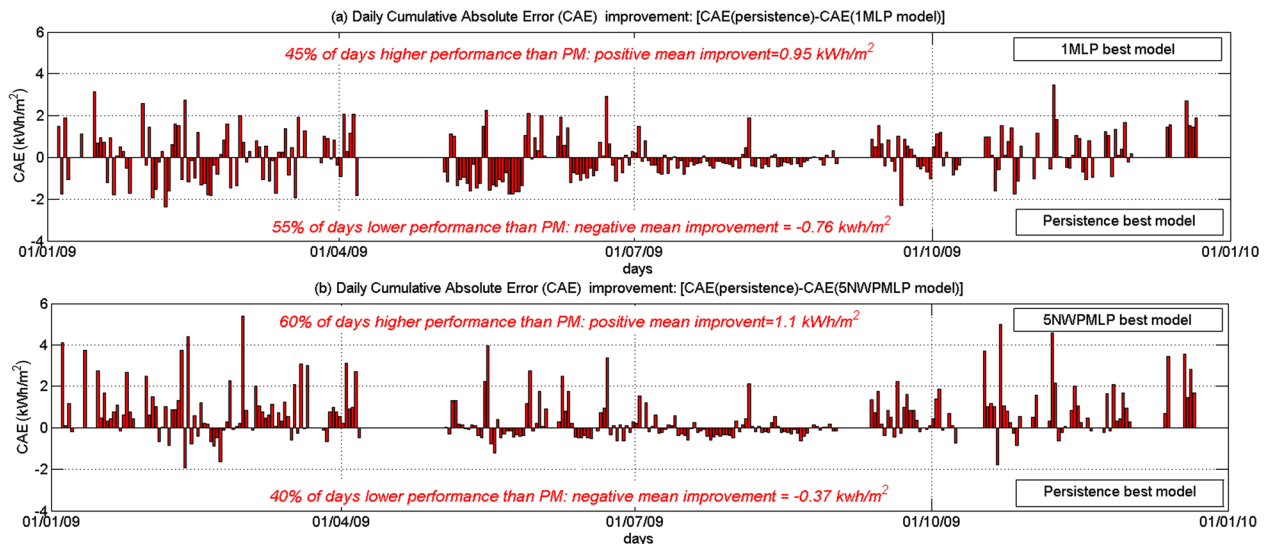


Fig. 5 Improvement 1MLP model (a) and 5NWPMLP model (b) with respect to the PM

the year and site should be done; thus, the results presented could not be generalized.

Four MOS approaches based on MLPNN architecture were developed and studied. All of them use NWP and local data as input and were trained with the site measured hourly POA irradiance. The 5NWPMLP model used as inputs both the local measured meteorological parameters: OD, H_{poa} , Ta, CR at lag0 and OD, and the NWP forecast daily irradiation: Hh_{nwp} at lag1. The 6NWPMLP model used directly the NWP predicted hourly horizontal irradiance: $Gh_{nwp_h}(t+1)$ (with $h=1,2,4$), while 7NWPMLP used both the meteorological parameters and the forecast NWP irradiance. Finally, the model 8NWPMLP used the two step approach: NWPMLP8.1 predicts the daily POA irradiation $H_{poa}(t+1)$ from the meteo parameters measured at day t and $t-1$ and Hh_{nwp} at $t+1$ while the described MLP4.2 shape forecast model reconstructs the $G_{poa}(t+1)$ from the forecast daily irradiation. All the approaches present an improvement up to 37%. Since the obtained results are all very similar, the increasing performance of the MOS techniques does not depend neither to local meteo parameters (input of 5NWPMLP) nor to NWP predicted hourly irradiance (input of 6NWPMLP). In any case, the best performance is obtained by 5NWPMLP. Figure 4 reports the scatter plot for this model.

Figure 5 reports the improvement in terms of daily cumulative absolute error (CAE) of the best ST and MOS models with respect to the PM: when the improvement is positive, the models produce smaller errors than the PM model while, when it is negative, the PM model provides a better forecast.

From Fig. 5(b), it appears that the MOS 5NWPMLP realizes, for the majority of the days, a great forecast improvement while only for few persistent days it provides a very small increase of the PM errors. Figure 6 compares the measured and forecast hourly trend for a sample of days for 1MLP and 5NWPMLP. The fast reaction of the MOS approach to the weather changing conditions due to the NWP irradiation forecast can be noted. On the whole, these MOS bring to high improvements: I_{RMSE} up to 37% and D_{NMAE} around 9% (see Table 4). From the reporting site an NMAE of 20.2% has been realized.

The high improvement of the MOS can be explained considering two different contributions coming from the NWP data and the ST correction. The main contribution of the NWP data is related to the good prediction of the daily horizontal irradiation while the contribution of the ST models using MLP is related to a best hourly prediction and to the irradiance transposition. Thus, the MOS improves the NWP hourly forecast and transposes the predicted horizontal irradiance on the POA.

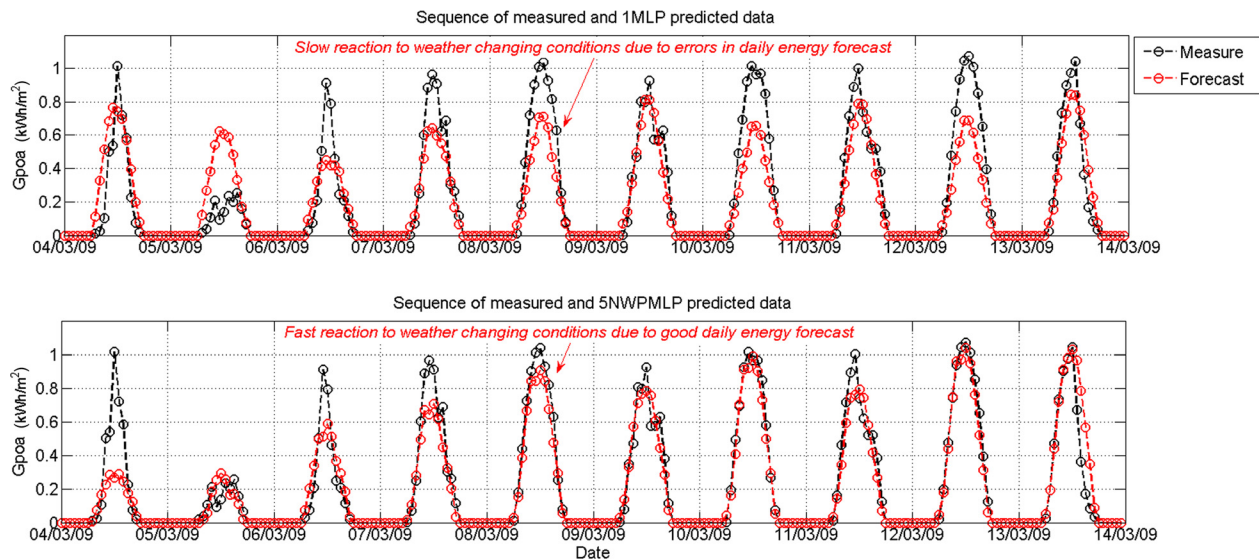


Fig. 6 Example of sequence of measured and forecast data for the 1MLP and the 5NWPMLP models

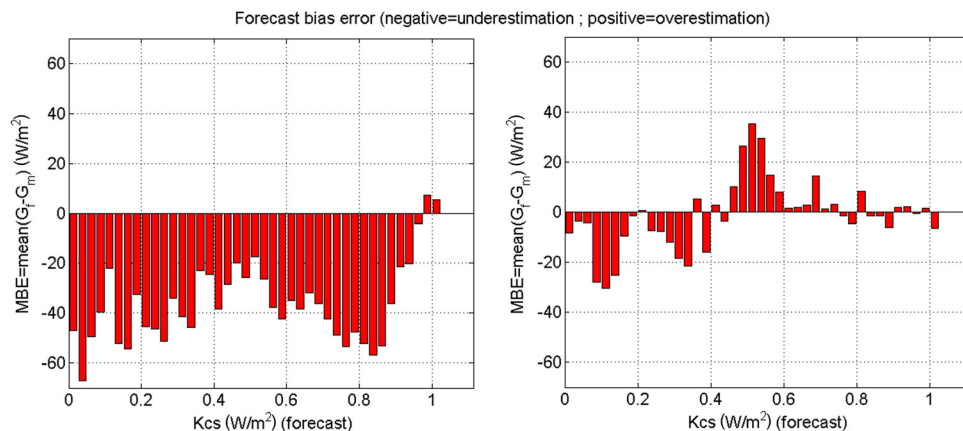


Fig. 7 On the left: MBE values versus forecast Kcs for the ECMWF; on the right: the same for the 5NWPMLP

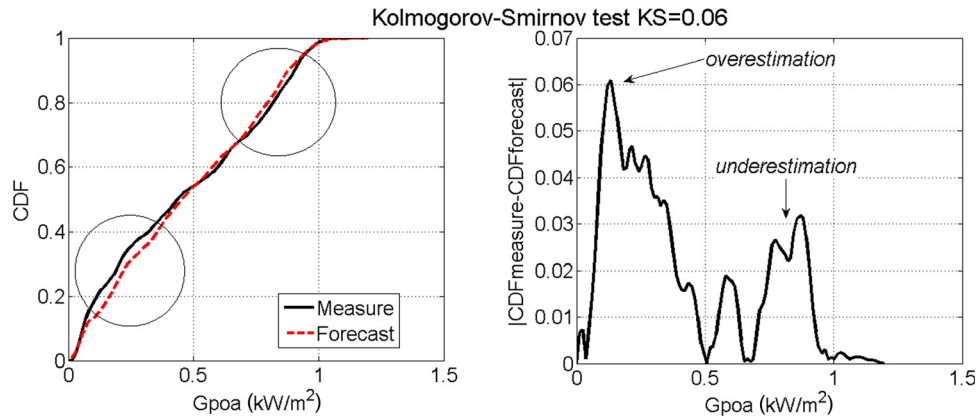


Fig. 8 5NWPMLP model KS test

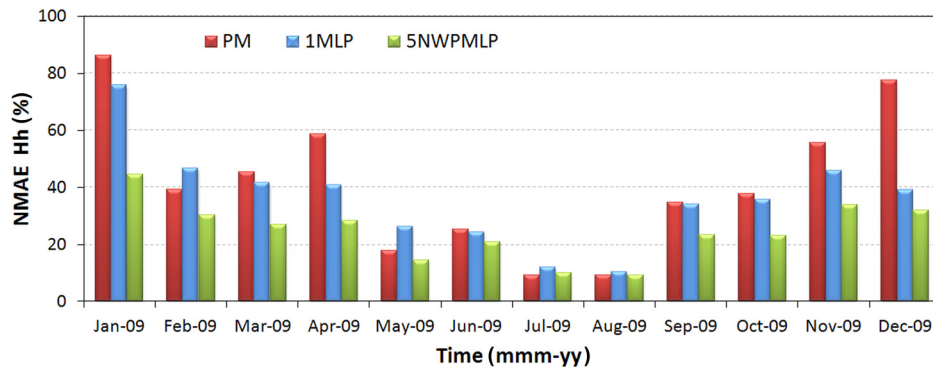


Fig. 9 Monthly performance of different forecast models

Table 5 Seasonal performance of the selected models. Bold-face values evidence the failure of ST model with respect to PM in spring and summer.

Season	NMAE H_{poa} (%)		
	1MLP	5NWPMLP	PM
Winter	50.6	30.6	50.2
Spring	28.5	19.3	25.5
Summer	15.1	12.8	14.0
Autumn	38.5	26.2	45.5

To evidence the benefit of the NWP and ST models combination (MOS approach) the mean bias error (MBE) trend with respect to the forecast clear sky index, K_{cs} is shown in Fig. 7 for the ECMWF prediction and the 5NWPMLP model, respectively. A consistent underestimation of solar irradiance is observed for the ECMWF prediction for all the forecast K_{cs} . This underestimation is smaller for forecast K_{cs} in the range of 0.4–0.6. 5NWPMLP reduces the negative ECMWF bias of almost 40 W/m^2 for forecast K_{cs} lower than 0.6 (cloudy and partially cloudy instants) and it almost eliminates the bias for forecast K_{cs} higher than 0.6 (partially cloudy to clear sky instants). The bias compensation for intermediate K_{cs} values results in an overestimation for 5NWPMLP. So the MOS main advantage consists in the bias reduction.

All the reported approaches exhibit an underestimation of the forecast value at high irradiance level and an overestimation at low irradiance level. This could be seen also from the measured and forecast CDF curves as reported in Fig. 8 for 5NWPMLP.

Figure 9 reports the monthly NMAE of the PM, 1MLP, and 5NWPMLP. All the models exhibit a lower performance with respect to the PM in the month of July and August; while 1MLP

Table 6 Sunny ($CR \leq 0.4$) and cloudy ($CR > 0.4$) days performance of the selected models

Model	NRMSE (%)		CORR	
	Sunny	Cloudy	Sunny	Cloudy
1MLP	37.1	44.5	0.83	0.78
5NWPMLP	28	34.9	0.91	0.87

Table 7 Not variable ($NM_{HV} \leq 0.4$) and variable ($NM_{HV} > 0.4$) days performance

Model	NRMSE (%)		CORR	
	Not variable	Variable	Not variable	Variable
1MLP	41.3	78.6	0.96	0.86
5NWPMLP	26	65.7	0.98	0.90

model also in February and May. Besides, from this figure, the small improvement of the ST model can be observed. From the seasonal point of view, the ST model fails in Summer and Spring time as evidenced in Table 5.

Finally, from Table 6, the difference between the performance of sunny and cloudy days can be observed. It should be noted that the NRMSE and CORR between sunny and cloudy days is greater than four points. Tables 7 and 8 report the comparison of the 1MLP and 5NWPMLP performance between variable and not variable days and between stable and unstable days. It appears that the performance difference between variable and not variable days is very similar: around 40% in NRMSE and ten points of correlation. On the contrary, the performance difference between

Table 8 Stable (NADV <= 0.4) and unstable (NADV <= 0.4) days performance

Model	NRMSE (%)		CORR	
	Stable	Unstable	Stable	Unstable
1MLP	39.6	118	0.96	0.77
5NWPMLP	32	87.6	0.97	0.87

stable and unstable days for the model 1MLP (ST) is almost 80% in NRMSE and 20 points in correlation (CORR in the table), while for the model 5NWPMLP (MOS) is almost 55% in NRMSE and ten points in correlation. Indeed, the MOS provides a much better irradiance forecast for unstable weather conditions, since the NWP data used for the model provide a good forecast of the daily irradiance. This could be observed also comparing the performance of the two 1MLP and 5NWPMLP; the NRMSE and CORR improvement is much smaller for stable days than for unstable days. Finally, it has to be pointed out that the NWP data used in the MOS are not operational forecast but a reanalysis. This fact could have improved the obtained results; however, it should not threaten the validity of the conclusions achieved due to the ability of ANN to use ground measurements to refine the forecast. Indeed, the improvement of the MOS could be more important using the operational NWP data than using the reanalysis. Further investigations will be done on this feature.

6 Conclusions

Several different POA irradiance forecast models on the 24 hr horizon have been developed using ANN algorithms. The performance of four ST models and four MOS approaches have been evaluated and discussed. The ST models use only site measured meteorological parameters as inputs, while the MOS is used to refine the input NWP data. The reference site is the University of Rome "Tor Vergata" and the reference year for the models test is 2009.

The used ST models show a performance in terms of RMSE improvement of around 20%. PM and ST models show the same results in terms of NMAE.

The MOS techniques correct NWP hourly forecast taking into account the site effects and transposing the predicted horizontal irradiance on the POA. Thus, they show the best performance increasing the improvement up to 37% in terms of RMSE and 9% in terms of NMAE. The annual imbalanced energy measure (NMAE) of these models is around 20%, very near to the Italian threshold of 15%.

In particular, the outperforming MOS solution is the 5NWPMLP, which is also the simplest approach.

For what concerns the amount of data used for this analysis, it has to be said that for MLP techniques 1 yr of training data are enough to provide an adequate accuracy of the forecast for the considered site. In any case, it should be remarked that the performance is strictly dependent on the persistence of the year used for testing.

Acknowledgment

The work presented was developed in the framework of the DSP project, funded by the 2010 MISE-ICE-CRUI agreement between the Italian Ministry of the Economic Development (MISE), the Italian Trade Promotion Agency (ICE), and the Conference of the Italian Rectors (CRUI). M. Pierro, F. Bucci, and M.

Taravat are supported by the same agreement. Thanks to Tecno El srl and Etexia srl that also funded the DSP project.

ECMWF ERA-40 (ECMWF Re-analysis) data used in this study have been provided by ECMWF. We gratefully acknowledge the PV Performance Modeling Collaborative website for providing some software libraries from PV_lib MATLAB Toolbox.

The ESTER facility is part of the Centre for Hybrid and Organic Solar Energy (CHOSE).

References

- [1] Kleissl, J., 2013, *Solar Energy Forecasting and Resource Assessment*, 1st ed., Academic Press.
- [2] Pelland, S., Remund, J., Kleissl, J., Oozeki, T., and De Brabandere, K., 2013, "Photovoltaic and Solar Forecasting: State of the Art," IEA PVPS, Task 14, Subtask 3.1, Report No. IEA-PVPS T14-01.
- [3] Muller, S. C., and Remund, J., 2010, "Advances in Radiation Forecast Based on Regional Weather Models MMF and WRF," Proceedings of the 25th EUPVSEC Conference 2010, Valencia, Spain, Sept. 6–9, pp. 4629–4632.
- [4] Perez, R., Kivalov, S., Schlemmer, J., Hemker, K., Jr., Renné, D., and Hoff, T. E., 2010, "Validation of Short and Medium Term Operational Solar Radiation Forecasts in the US," *Sol. Energy*, **84**(12), pp. 2161–2172.
- [5] Martin, L., Zarzalejo, L. F., Polo, J., Navarro, A., Marchante, R., and Cony, M., 2010, "Prediction of Global Solar Irradiance Based on Time Series Analysis: Application to Solar Thermal Power Plants Energy Production Planning," *Sol. Energy*, **84**(10), pp. 1772–1781.
- [6] Mellit, A., and Massi Pavan, A., 2010, "A 24-h Forecast of Solar Irradiance Using Artificial Neural Network: Application for Performance Prediction of a Grid-Connected PV Plant in Trieste, Italy," *Sol. Energy*, **84**(5), pp. 807–821.
- [7] Voyant, C., Randimivololona, P., Nivet, M. L., Poli, C., and Muselli, M., 2013, "Twenty Four Hours Ahead Global Irradiation Forecasting Using Multi-Layer Perceptron," *Meteorol. Appl.*, **21**(3), pp. 644–655.
- [8] Wang, F., Mi, Z., Su, S., and Zhao, H., 2012, "Short-Term Solar Irradiance Forecasting Model Based on Artificial Neural Network Using Statistical Feature Parameters," *Energies*, **5**(5), pp. 1355–1370.
- [9] Guarnieri, R. A., Pereira, E. B., and Chou, S. C., 2006, "Solar Radiation Forecast Using Artificial Neural Networks in South Brazil," Proceedings of the 8th ICSHMO 2006, Foz do Iguaçu, Brazil, Apr. 24–28, pp. 1777–1785.
- [10] Chen, C., Duan, S., Cai, T., and Liu, B., 2011, "Online 24-h Solar Power Forecasting Based on Weather Type Classification Using Artificial Neural Network," *Sol. Energy*, **85**(11), pp. 2856–2870.
- [11] Lorenz, E., Hurka, J., Heinemann, D., and Beyer, H. G., 2009, "Irradiance Forecasting for the Power Prediction of Grid Connected Photovoltaic Systems," *IEEE J. Sel. Top. Appl. Earth Obs. Remote Sens.*, **2**(1), pp. 2–10.
- [12] Lorenz, E., Remund, J., Müller, S. C., Traunmüller, W., Steinmaurer, G., Pozo, D., Ruiz-Arias, J. A., Fanego, V. L., Ramirez, L., Romeo, M. G., Kurz, C., Pomares, L. M., and Guerrero, C. G., 2009, "Benchmarking of Different Approaches to Forecast Solar Irradiance," Proceedings of the 24th European Photovoltaic Solar Energy Conference, Germany, Hamburg, Sept. 21–25, pp. 4199–4208.
- [13] Pedro, H. T. C., and Coimbra, C. F. M., 2012, "Assessment of Forecasting Techniques for Solar Power Production With No Exogenous Inputs," *Sol. Energy*, **86**(7), pp. 2017–2028.
- [14] Lorenz, E., Heinemann, D., Wickramaratne, H., Beyer, H., and Bofinger, S., 2007, "Forecast of Ensemble Power Production by Grid-Connected PV Systems," Proceedings of the 20th EUPVSEC, Milano, Italy, Sept. 3–7.
- [15] Dee, D. P., Uppala, S. M., Simmons, A. J., Berrisford, P., Poli, P., Kobayashi, S., Andrae, U., Balmaseda, M. A., Balsamo, G., Bauer, P., Bechtold, P., Beljaars, A. C. M., van de Berg, L., Bidlot, J., Bormann, N., Delsol, C., Dragani, R., Fuentes, M., Geer, A. J., Haimberger, L., Healy, S. B., Hersbach, H., Hólm, E. V., Isaksen, I., Kållberg, P., Köhler, M., Matricardi, M., McNally, A. P., Monge-Sanz, B. M., Morcrette, J.-J., Park, B.-K., Peubey, C., de Rosnay, P., Tavolato, C., Thépaut, J.-N., and Vitart, F., 2011, "The ERA-Interim Reanalysis: Configuration and Performance of the Data Assimilation System," *Q. J. R. Meteorol. Soc.*, **137**(656), pp. 553–597.
- [16] Spena, A., Cornaro, C., and Serafini, S., 2008, "Outdoor ESTER Test Facility for Advanced Technologies PV Modules," Proceedings of the 33rd IEEE Photovoltaic Specialists Conference, San Diego, CA, May 11–16, pp. 1–5.
- [17] Zahumenský, I., 2004, *Guidelines on Quality Control Procedures for Data From Automatic Weather Stations*, World Meteorological Organization, Switzerland.
- [18] Marquez, R., and Coimbra, C. F. M., 2011, "Forecasting of Global and Direct Solar Irradiance Using Stochastic Learning Methods, Ground Experiments and the NWS Database," *Sol. Energy*, **85**(5), pp. 746–756.
- [19] Beyer, H. G., Polo Martinez, J., Suri, M., Torres, J. L., Lorenz, E., Müller, S. C., Hoyer-Klick, C., and Ineichen, P. D., 2009, "Report on Benchmarking of Radiation Products," MESoR, Report No. 038665, pp. 108–111.
- [20] Bishop, C. M., 1995, *Neural Network for Pattern Recognition*, Clarendon Press, Oxford, UK, p. 290.